SUPPLEMENTAL MATERIAL

Raman Hyperspectral Imaging with Multivariate Analysis for Investigating Enzyme Immobilization

Joseph P. Smith[1*], Melinda Liu[1], Mackenzie L. Lauro[1], Madhumitha Balasubramanian[2], Jacob H. Forstater[3], Shane T. Grosser[3], Zachary E.X. Dance[1], Timothy A. Rhodes[2], Xiaodong Bu[1], Karl S. Booksh[4]

[1]Analytical Research & Development, MRL, Merck & Co., Inc., Rahway, NJ 07065

[2]Pharmaceutical Sciences, MRL, Merck & Co., Inc., Rahway, NJ 07065

[3]Small Molecule Process Research & Development, MRL, Merck & Co., Inc., Rahway, NJ 07065

[4]Department of Chemistry & Biochemistry, University of Delaware, Newark, DE 19716

[*]Corresponding Author:

Joseph P. Smith. Tel: (732) 594-0194. Email: joseph.smith@merck.com

RESULTS AND DISCUSSION

S1. RAMAN SPECTRA OF REFERENCE MATERIALS FOR ENZYME IMMOBILIZATION. Reference materials of chemical species used during this enzyme immobilization process (**Section 2.1**) were analyzed using Raman microspectroscopy. Raman spectra were collected using both 532 nm and 785 nm excitation. Raman bands observed for pantothenate kinase (PanK), the acrylamide-based resin, and the methacrylate-based resin with the chemical assignment and relevant literature is outlined (**Table S1**, Supplemental Material).

Raman Band (cm^{-1})	Chemical Identity	Laser Excitation (nm)	Assignment	Relevant Literature
1004	PanK	532	phenylalanine	1, 2
1131	PanK	532	tryptophan	1, 2
1343	PanK	532 & 785	tryptophan	1, 2
1454	PanK	532	deformation of C-H bonds	1, 2
1662	PanK	532	amide I region	1, 2
1003	PanK	785	phenylalanine	1, 2
1448	PanK	785	deformation of C-H bonds	1, 2
1664	PanK	785	amide I region	1, 2
902	Acrylamide	532	C-C symmetrical stretching	3
1112	Acrylamide	532	C-C asymmetrical stretching	3
1306	Acrylamide	532	C-H deformation	3
1451	Acrylamide	532	C-H deformation	3
1660	Acrylamide	532	amide-based C=O stretching	3
905	Acrylamide	785	C-C symmetrical stretching	3
1111	Acrylamide	785	C-C asymmetrical stretching	3
1304	Acrylamide	785	C-H deformation	3
1453	Acrylamide	785	C-H deformation	3
1661	Acrylamide	785	amide-based C=O stretching	3
603	Methacrylate	532	C-C-O stretching	4, 5, 6, 7
807	Methacrylate	532	-$COOCH_3$ stretching	4, 5, 6, 7
1119	Methacrylate	532	C-C asymmetrical stretching	3
1259	Methacrylate	532	C-O stretching	4, 5, 6, 7
1428	Methacrylate	532	-$COOCH_3$ stretching	4, 5, 6, 7
1454	Methacrylate	532	-$COOCH_3$ stretching	4, 5, 6, 7
1729	Methacrylate	532	C=O esters	4, 5, 6, 7
838	Methacrylate	785	-CH_2 stretching	4, 5, 6, 7
1116	Methacrylate	785	C-C asymmetrical stretching	3
1263	Methacrylate	785	C-O stretching	4, 5, 6, 7
1427	Methacrylate	785	-$COOCH_3$ stretching	4, 5, 6, 7
1457	Methacrylate	785	-$COOCH_3$ stretching	4, 5, 6, 7

1726	Methacrylate	785	C=O esters	4, 5, 6, 7

NOTE: *PanK = pantothenate kinase; Acrylamide = acrylamide-based resin (Ni-nitrilotriacetic acid (NTA) immobilized metal affinity chromatography (IMAC) resin), Methacrylate = methacrylate-based resin (Ni-iminodiacetic acid (IDA) resin).*

Raman spectra of reference materials were collected using both 532 nm and 785 nm excitation (**Figure S1**). In total, five reference materials were analyzed—lyophilized powder of pantothenate kinase, acrylamide resin, methacrylate resin, Bis-Tris solid, and glass substrate.

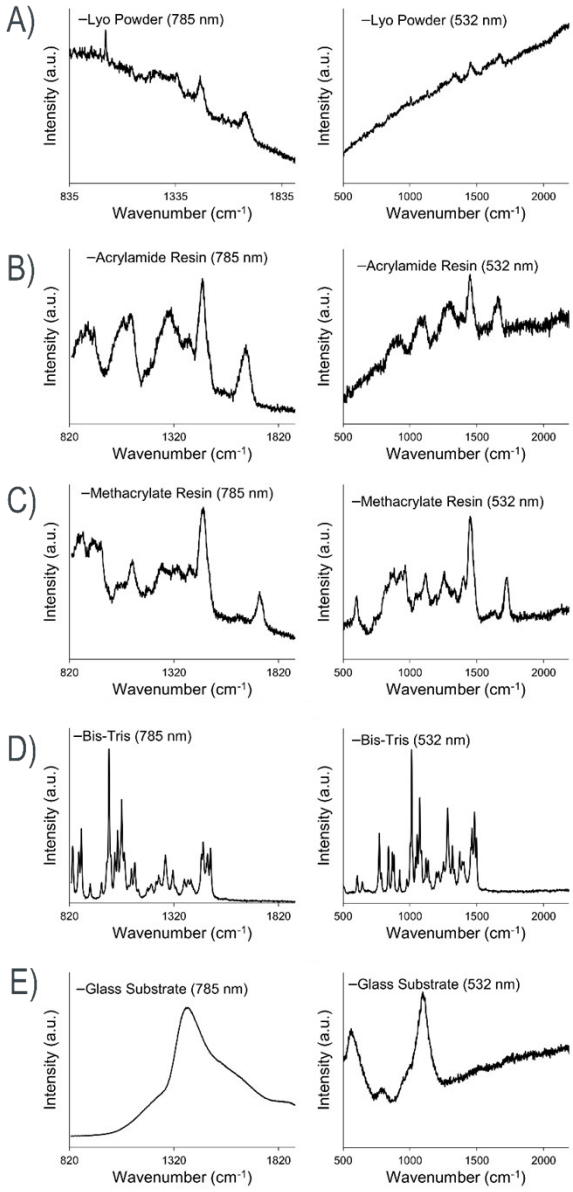

Figure S1: Raman Spectra of reference materials used during the enzyme immobilization process collected using both 532 nm and 785 nm excitation: (a) lyophilized powder of pantothenate kinase (PanK); (b) acrylamide resin; (c) methacrylate resin; (d) Bis-Tris solid; (e) glass substrate.

S2. MULTIVARIATE ANALYSIS APPLIED TO RAMAN HYPERSPECTRAL IMAGING DATA OF IMMOBILIZED ENZYMES USING PRINCIPAL COMPONENT ANALYSIS (PCA). Raman hyperspectral imaging with principal component analysis (PCA) of pantothenate kinase (PanK) immobilized to acrylamide resin (**Figure S2**) resolves the spatial distribution and corresponding chemical identity both enzyme and resin. The optical image (**Figure S2a**) shows three ~50 μm diameter acrylamide beads. A total of 3660 spectra were collected (60 by 61 spectral grid) using 532 nm excitation. The mean Raman spectrum (**Figure S2a**) shows distinct Raman bands at 1451 cm^{-1} and 1662 cm^{-1} characteristic of primarily acrylamide resin.

Results of PCA applied to Raman hyperspectral imaging (**Figure S2**) are displayed with PCA-resolved scores as chemical images shown in the left column with corresponding PCA-resolved loadings shown in the right column. The resolved loadings for the first principal component (**Figure S2b**) display intense Raman bands at 1451 cm^{-1} and 1662 cm^{-1} with additional Raman bands at 890 cm^{-1} and 1108 cm^{-1} that are all characteristic of acrylamide resin. The resolved loadings for the second principal component (**Figure S2c**) display Raman bands at 1001 cm^{-1} and 1665 cm^{-1} that are characteristic of PanK.

The spatial distribution of the acrylamide resin (**Figure S2b**) demonstrate agreement with the three bead locations in the corresponding optical image (**Figure S2a**), in which higher acrylamide abundance is observed towards the boundary of the beads. The spatial distribution of PanK (**Figure S2c**) shows an enzyme distribution throughout all resin beads, in which the enzyme appears to be more concentrated towards the center of the beads. Given the resolved loading of the enzyme is lower signal-to-noise than that of the resin, the respective chemical image is also lower signal-to-noise, as observed in **Figure S2**.

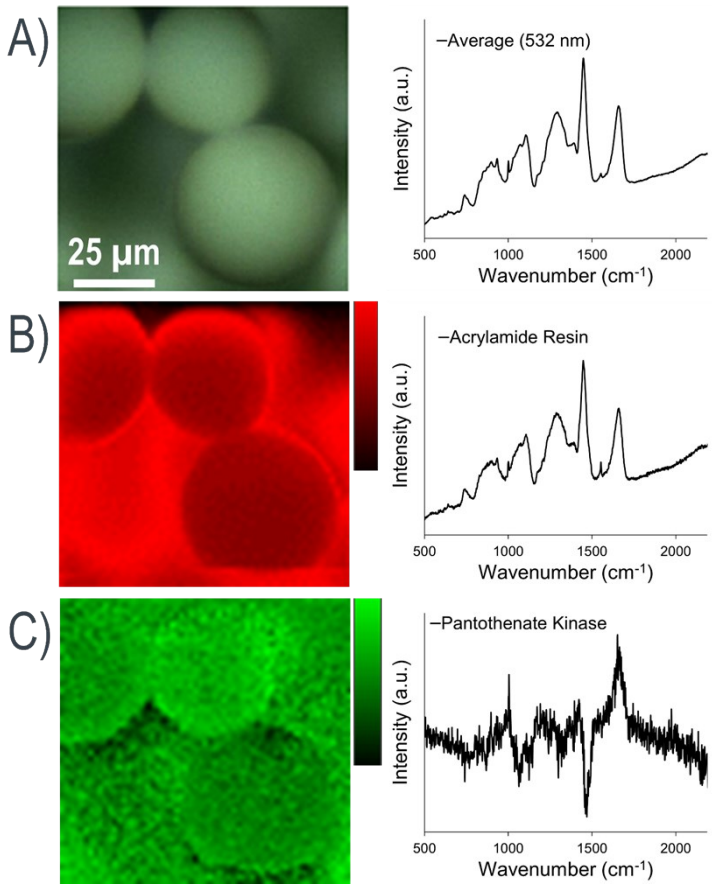

Figure S2: Principal component analysis (PCA) applied to Raman hyperspectral imaging, collected with 532 nm excitation, of pantothenate kinase (PanK) immobilized onto acrylamide resin. The optical image (a), mean Raman spectrum (a), scores (left, b-c), and loadings (right, b-c) are shown for each resolved principal component (PC). The first PC was identified as acrylamide resin (b) and the second PC was identified as PanK (c).

Raman hyperspectral imaging with PCA of PanK immobilized to a methacrylate resin (**Figure S3**) resolves the spatial distribution and corresponding chemical identity of three principal components—methacrylate resin, Bis-Tris, and PanK. The optical image (**Figure S3a**) shows one single ~100 µm methacrylate bead. A total of 3192 spectra were collected (56 by 67 spectral grid) using 785 nm excitation. The mean Raman spectrum (**Figure S3a**) shows distinct Raman bands characteristic of primarily resin (1459 cm^{-1}) and enzyme (1003 cm^{-1}).

The resolved loadings for the first principal component (**Figure S3b**) display Raman bands at 875 cm^{-1}, 1007 cm^{-1}, 1278 cm^{-1}, 1459 cm^{-1}, and 1730 cm^{-1} characteristic of methacrylate. The resolved loadings for the second principal component (**Figure S3c**) display intense Raman bands at 1007 cm^{-1}, 1068 cm^{-1}, and 1492 cm^{-1} with several additional, less intense Raman bands throughout the spectral range, that are characteristic of Bis-Tris. The resolved loadings for the third principal component (**Figure S3d**) display an intense Raman bands at 1003 cm^{-1} characteristic of PanK.

The spatial distribution of the methacrylate resin (**Figure S3b**) demonstrate that methacrylate is distributed throughout the bead location, in agreement with the optical image (**Figure S3a**). The spatial distribution of Bis-Tris (**Figure S3c**) shows this chemical species is

distributed throughout the resin bead, with low abundance towards the bottom-right portion of the bead. The spatial distribution of PanK (**Figure S3d**) shows an enzyme distribution throughout most of the resin beads, with high abundance towards the left portion of the resin and low abundance towards the top-right and bottom-right portions of the bead.

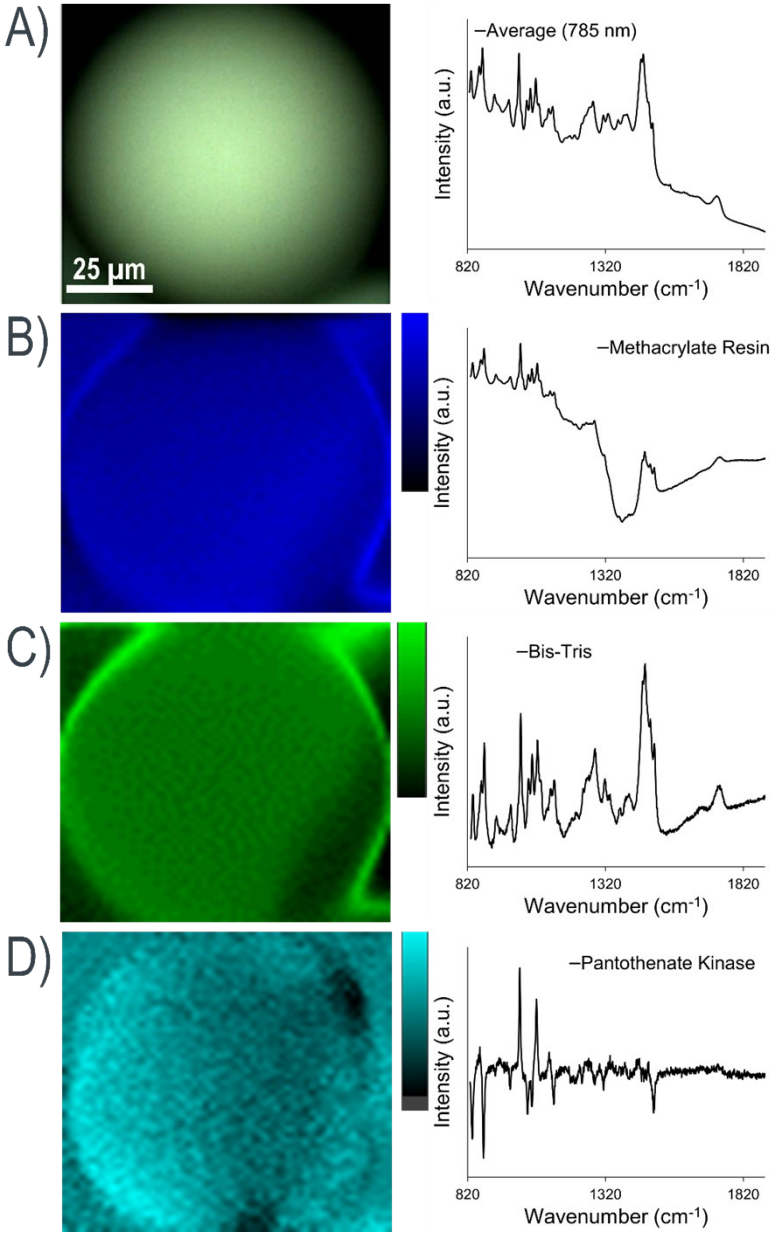

Figure S3: Principal component analysis (PCA) applied to Raman hyperspectral imaging, collected with 785 nm excitation, of pantothenate kinase (PanK) immobilized onto methacrylate resin. The optical image (a), mean Raman spectrum (a), scores (left, b-d), and loadings (right, b-d) are shown for each resolved principal component (PC). The first PC was identified as acrylamide resin (b), the second PC was identified as Bis-Tris (c), and the third PC was identified as PanK (d).

For the development and application of an innovative analytical methodology using Raman hyperspectral imaging with multivariate analysis to investigate enzyme immobilization, excitation wavelength is an important acquisition parameter to evaluate. This is due in part to Raman signal being inversely proportional to the fourth power of the excitation wavelength. In addition to this, the observed Raman signal can change significantly with respect to excitation wavelength and is based on the scattering efficiency profile, the instrumental optics, and the detector. In practice, advantages can be harnessed by selecting the optical excitation wavelength. For example, the primary advantage of 532 nm excitation is strong signal intensity, whereas the primary disadvantage is fluorescence background interference, which affects the shot noise and observed Raman scattering. The primary advantage of 785 nm excitation is limited fluorescence interference effects, whereas the primary disadvantage is weak signal intensity, which is intuitive given signal intensity is inversely proportional to the fourth power of excitation wavelength. As demonstrated in this work, 785 nm excitation generally outperformed 532 nm excitation for investigating PanK immobilization, an important observation for methodology development.

This work demonstrated the ability for Raman hyperspectral imaging in conjunction with PCA to probe chemically-diverse resin beads to enable process development of enzyme immobilization. Multiple resins beads were interrogated to provide a general assessment of the immobilization process. This methodology can potentially provide critical chemical criteria of the immobilization, such as the enzyme coverage of resins or the number of resin beads that contain enzyme, helping to determine the success of an enzyme immobilization process. Raman hyperspectral imaging in conjunction with PCA also enabled detailed characterization of enzyme immobilized in individual resin beads. Information concerning the enzyme immobilization, including spatial distributions, locations of enzyme relative to resin, or detailed chemical information concerning the interaction of the enzyme and resin, can be obtained using this methodology. Therefore, this novel analytical methodology can now be more broadly applied to determine spatial, chemical, and molecular information critical to the development and characterization of biocatalysts and other immobilization modalities, including immobilized proteins for clinical diagnostics, improved Protein A resins for monoclonal antibody purification, and resin biofouling.

REFERENCES:

1. Tuma, R., Raman spectroscopy of proteins: from peptides to large assemblies. *Journal of Raman Spectroscopy* **2005**, 36 (4), 307-319.
2. Wen, Z. Q., Raman spectroscopy of protein pharmaceuticals. *Journal of Pharmaceutical Sciences* **2007**, 96 (11), 2861-2878.
3. Murugan, R.; Mohan, S.; Bigotto, A., FTIR and polarised Raman spectra of acrylamide and polyacrylamide. *Journal of the Korean Physical Society* **1998**, 32 (4), 505-512.
4. Carrasco-Correa, E. J.; Ramis-Ramos, G.; Herrero-Martinez, J. M., Methacrylate monolithic columns functionalized with epinephrine for capillary electrochromatography applications. *Journal of Chromatography A* **2013**, 1298, 61-67.
5. Sharma, J.; Ahuja, S.; Arya, R. K., Depth profile study of poly(styrene) - poly(methyl methacrylate) - tetrahydrofuran coatings. *Progress in Organic Coatings* **2019**, 134, 297-302.
6. Hosseini, S.; Ibrahim, F.; Rothan, H. A.; Yusof, R.; van der Marel, C.; Djordjevic, I.; Koole, L. H., Aging effect and antibody immobilization on -COOH exposed surfaces designed for dengue virus detection. *Biochemical Engineering Journal* **2015**, 99, 183-192.
7. Thomas, K. J.; Sheeba, M.; Nampoori, V. P. N.; Vallabhan, C. P. G.; Radhakrishnan, P., Raman spectra of polymethyl methacrylate optical fibres excited by a 532 nm diode pumped solid state laser. *Journal of Optics a-Pure and Applied Optics* **2008**, 10 (5), 5.